



Tracing solute sources and carbon dynamics under various hydrological conditions in a karst river in southwestern China

Jing Liu¹ · Bo Chen² · Zhu-Yan Xu¹ · Yuan Wei¹ · Zhi-Hua Su¹ · Rui Yang¹ · Yong-Xue Ji¹ · Xiao-Dan Wang³ · Li-Li Zhang⁴ · Ning An⁵ · Fei Yang⁵

Received: 26 August 2019 / Accepted: 7 January 2020
© Springer-Verlag GmbH Germany, part of Springer Nature 2020

Abstract

Understanding the mechanisms that lead various hydrological conditions to influence solute and carbon dynamics in karst rivers is a crucial issue. In this study, high-frequency sampling and analyses of water chemistry and $\delta^{13}\text{C}_{\text{DIC}}$ were conducted from October 2013 to September 2014 in a typical karst river, the Beipan River in southwestern China. The major ions (such as Ca^{2+} , Mg^{2+} , HCO_3^- , K^+ , SO_4^{2-} , Na^+ , and Cl^-) in the river are mainly from the weathering of carbonates and silicates and present temporal hydrological variabilities. Sr and U are mainly derived from carbonate weathering and show chemostatic behaviors responding to increasing discharge, similar to carbonate-sourced ions Ca^{2+} , Mg^{2+} , and HCO_3^- . Silicate weathering is the primary source of Al and Li, which show significant dilution effects similar to those of Na^+ responding to high discharge. Meanwhile, most dissolved trace elements (such as Zn, Cu, Ba, Sb, Mn, Mo, and Pb) are strongly impacted by anthropogenic overprints and also exhibit a significant seasonal variability, which may be related with mining activities in the investigated area. A simultaneous increase of $\delta^{13}\text{C}_{\text{DIC}}$ and decrease in ΔDIC contents and $p\text{CO}_2$ values suggests that photosynthesis is the primary control on riverine DIC variability during the high-flow season. Besides, the $p\text{CO}_2$ values display significant chemostatic behaviors owing to the influx of biological CO_2 , which is produced by microbiological activities and ecological processes, and enhanced by monsoonal climatic conditions. A two-dimensional endmember mixing model demonstrates that carbonate weathering (averaging 62%) along with biological carbon (averaging 38%) are main sources to the riverine DIC, with temporal variability. Consequently, these results show that carbonate weathering and involved plant photosynthesis are the dominant processes controlling the riverine DIC contents under high discharge and temperature conditions. This work provides insight into the crucial influence of hydrological variability on solute sources and carbon dynamics under monsoonal climate for the karst rivers.

Keywords Major ions · Trace elements · Carbon dynamics · Hydrological variability

Responsible editor: Philippe Garrigues

✉ Jing Liu
liujingaiskl@hotmail.com

¹ School of Management Science, Guizhou University of Finance and Economics, Guiyang 550025, China

² School of Public Management, Guizhou University of Finance and Economics, Guiyang 550025, China

³ School of Eco-Environment Engineering, Guizhou Minzu University, Guiyang 550025, China

⁴ School of Geography and Resources, Guizhou Education University, Guiyang 550018, China

⁵ The State Key Laboratory of Environmental Geochemistry, Institute of Geochemistry, Chinese Academy of Sciences, Guiyang 550081, China

Introduction

River system plays a significant role in providing terrestrial weathering loads from the continent to the ocean (Juhlke et al. 2019; Li and Bush 2015; Li Yung Lung et al. 2018). Riverine solutes and carbon cycling are controlled by chemical and physical erosions, climatic conditions, and human activities at catchment; at the global scale, they can regulate the Earth's long-term climate change through complicated biogeochemical processes (Cox et al. 2000; Krishna et al. 2018; Pant et al. 2018; Rai et al. 2010). Hydrological processes are dominant drivers for solutes and carbon dynamics (Colombo et al. 2018; Maher and Chamberlain 2014; Schulte et al. 2011). The hydrochemistry in river waters enable the processes of chemical and physical erosions of the catchment to be traced (Rai et al. 2010; Zakharova et al. 2005). Meanwhile, the

temporal variations of trace elements responding to hydrological conditions have also been extensively studied in catchments because of their significant impact on recreating the history of chemical weathering processes (Colombo et al. 2018; Correa et al. 2019; Gaillardet et al. 1997; Yang et al. 2009) and because of their influence on aquatic ecosystems and human health (Chen et al. 2014; Qu et al. 2019). This is especially true for draining mine lands.

Riverine carbon dynamics are controlled by the combined effects of water–gas exchange, the weathering of minerals, and ecological processes, particularly the photosynthesis/respiration of subaquatic plants (or primary producers), which can be significantly impacted by monsoonal climate variabilities (Amaral et al. 2018; Brunet et al. 2009; Doctor et al. 2008; Li 2018; Shin et al. 2011). Dissolved inorganic carbon (DIC) is a major constituent of carbon species and accounts for ~38% of the total fluvial carbon transport to the oceans (approximately 1 Pg C/year) (Gaillardet et al. 1999). The major sources of DIC in river water include the weathering of carbonates and silicates, soil respired CO₂, and water–gas exchanges in the catchment (Dessert et al. 2003; Duvert et al. 2018; Gaillardet et al. 1999; Krishna et al. 2018; Li et al. 2008; Tamooh et al. 2013; Viers et al. 2014). Previous studies have shown that the riverine solute content–discharge relationships can be useful to understand the solute sources and carbon dynamics in river systems (Li and Bush 2015; McClanahan et al. 2016; Waldron et al. 2007; Zhong et al. 2018; Zhong et al. 2017b). For instance, in the high-flow season, changes the groundwater flow paths to shallow subsurface flow paths affect physical and biological processes in river systems, which could subsequently alter the carbon mix-endmembers compositions (Waldron et al. 2007). To better understand how the carbon dynamics respond to various hydrological conditions, $\delta^{13}\text{C}_{\text{DIC}}$ has been used to qualify and quantify the source and evolution of inorganic carbon in rivers (Li et al. 2008; Li et al. 2010; McClanahan et al. 2016; Poulson and Sullivan 2010; Zhong et al. 2018; Zhong et al. 2017b).

The Beipan River catchment in the Guizhou Province, southwestern China, is located in the center of the Southeast Asian Karst Region, which is the largest karst area in the world with a typical monsoonal climate. It is an ideal study object for tracing dissolved solutes transport and riverine DIC dynamics in response to hydrological variability in monsoonal areas. In this study, we show that major and trace elements along with carbon isotopes of DIC in river water, which can be used to evaluate the behaviors of solutes and to qualify and quantify the riverine DIC sources impacted by climatic variability through time series of sampling and analyses. The ultimate purpose is to explore the water–rock coupling mechanisms as well as controls of relevant biogeochemical processes under various climatic conditions for karst rivers.

Study area

The Beipan River catchment lies in the center of the Southeast Asian Karst Region, the largest karst area in the world with a typical monsoonal climate (Li et al. 2008; Xu and Liu 2007). It is one of the largest tributaries of the Xijiang River (Pearl River) in the upper reaches, with an area of 26,590 km² (Fig. 1). It is exposed to a seasonal monsoonal climate, with mean annual precipitation of 1286.3 mm and mean annual temperature of 16.6 °C. In terms of lithology, the study area is mostly occupied by Permian and Triassic carbonate strata and coal-bearing formations with high quantities of sulfides. Igneous and detrital sedimentary rocks constitute the other lithologies (Han and Jin 1996).

Materials and methods

The sampling location was located at the outlet of the Beipan River (Fig. 1), approximately 42 km away from the mainstream of the Xijiang River. The water samples for chemical and isotopic analyses were collected monthly in a hydrological year ranging from October 2013 to September 2014. Additionally, daily or weekly water samples were collected in the high-flow season from June to September 2014 on the basis of hydrological conditions. The river water samples were collected in the middle of the river using 10 L high-density polyethylene container and immediately filtered through Millipore nitrocellulose membrane filters. Two filtered solutes were prepared: one for cations and trace elements were acidified to a pH < 2 with ultra-purified HNO₃ and another was stored directly in a polyethylene bottle for anion analyses. All containers for stored water samples were pre-washed with high-purity HCl and rinsed with Milli-Q water (18.2 MΩ cm). All samples were stored in a refrigerator at 4 °C until analysis.

Alkalinity was determined by titration using 0.02 M HCl within 24 h of sample collection. Anions (Cl⁻, SO₄²⁻, and NO₃⁻) were analyzed by ionic chromatography within a precision of 5% while major cations (K⁺, Na⁺, Ca²⁺, and Mg²⁺) and Si were analyzed by inductively coupled plasma-optical emission spectrometry (ICP-OES), at a precision better than 3%. Trace elements were analyzed by Agilent Technologies 7700 Series ICP-MS. The quality of the analyses was controlled by adding an external standard (Th) and regular international SLRS5 standards, with the discrepancy between triplicates being less than 5%. For the stable isotopic compositions ($\delta^{13}\text{C}$) of dissolved inorganic carbon (DIC) analyses, the method of Li et al. (2010), with a precision of 0.1% was used. All these analyses were conducted in the State Key Laboratory of Environmental Geochemistry, Institute of Geochemistry, Chinese Academy of Science. Daily water discharge data (m³/s) were obtained online from the Ministry of Water Resources (<http://www.hydroinfo.gov.cn/>).

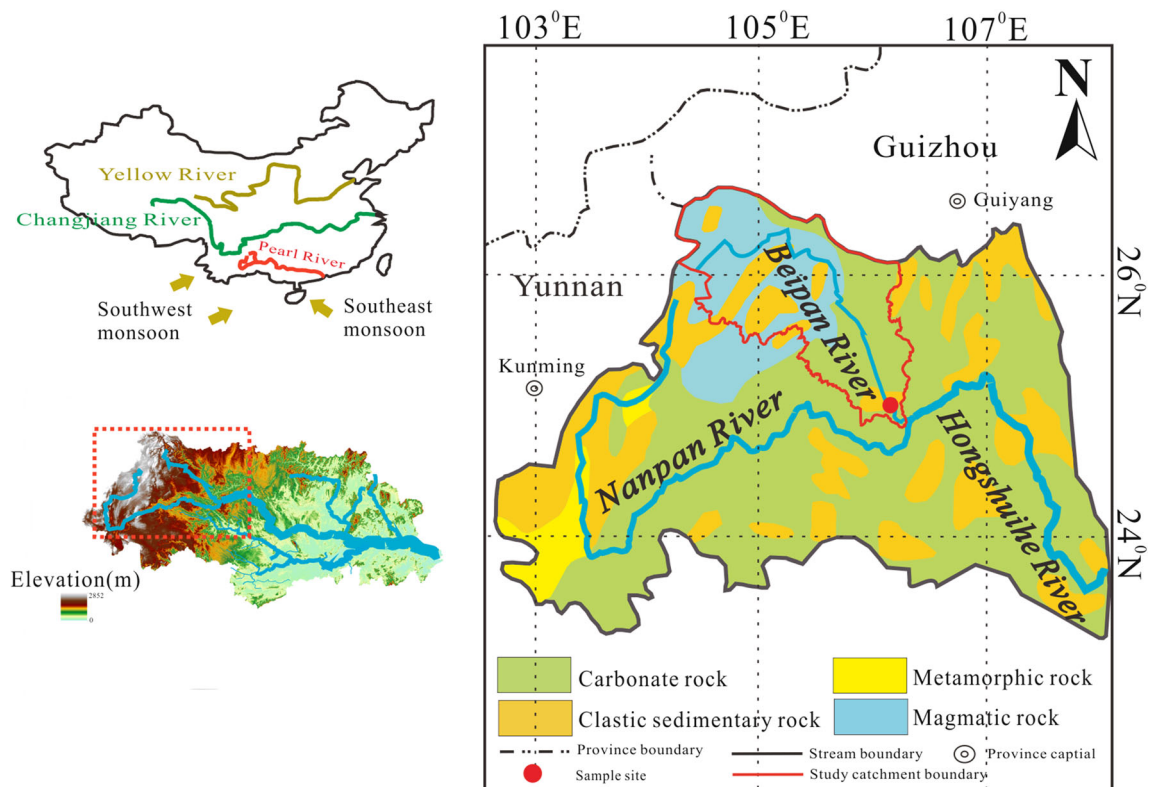


Fig. 1 Sampling location and geological background of the Beipan River

Results

Temporal variations of hydrochemical characteristics

The Beipan River water was mildly alkaline within the hydrological year, with pH values increased from 7.9 in the high-flow season to 8.4 in the low-flow season. The temperature of the river water ranged from 11.2 to 22.8 °C, for a mean value of 19.1 °C. The total cationic charge ($TZ^+ = K^+ + Na^+ + Ca^{2+} + Mg^{2+}$) and total dissolved anionic charge ($TZ^- = HCO_3^- + Cl^- + NO_3^- + SO_4^{2-}$) were well balanced, with all NICB ($NICB = (TZ^+ - TZ^-) \times 100\% / (TZ^+ + TZ^-)$) below 5%. The total dissolved solids ($TDS = K^+ + Na^+ + Ca^{2+} + Mg^{2+} + HCO_3^- + Cl^- + NO_3^- + SO_4^{2-} + SiO_2$, mg/l) ranged from 195 to 311 mg/l, with an average of 262 mg/l, which is significantly higher than the world average value of 97 mg/l (Li and Bush 2015). The base cation contents ranged from 923 to 1432 μM for Ca^{2+} , 256–534 μM for Mg^{2+} , 121–365 μM for Na^+ , and 27–56 μM for K^+ , while the major anion contents ranged from 1806 to 2675 μM for HCO_3^- , 240–752 μM for SO_4^{2-} , 75–312 μM for NO_3^- , and 55–176 μM for Cl^- . The study river clearly possessed high contents of Ca^{2+} , Mg^{2+} , and HCO_3^- , which is consistent with the typical characteristics of carbonate-dominated rivers (Jiang et al. 2018; Li et al. 2008; Xu and Liu 2007; Zhong et al. 2017b).

Sr, Al, Ba, and Li are the main components of dissolved trace elements, and their contents ranged between

1391 and 5909 nM for Sr, 164–1258 nM for Al, 110–331 nM for Ba, and 38–274 nM for Li, which is significantly higher than those of other trace elements. Sr (averaging 3617 nM) and Sb contents (averaging 22 nM) in the Beipan River are significantly higher than the world average contents of 684 nM and 0.6 nM, respectively (Gaillardet and Dupré 2005), while U, Pb, and Co contents are relatively low in the Beipan River during the study period.

Carbon species and isotopic compositions of DIC

Riverine DIC content is the sum of the aqueous carbon dioxide (CO_2 (aq)), carbonic acid (H_2CO_3), bicarbonate (HCO_3^-), and carbonate (CO_3^{2-}) ion contents (Li et al. 2010), varying from 1840 to 2744 μM , for an average of 2254 μM in the Beipan River, which is nearly threefold higher than the world average content of 852 μM (Voss et al. 2014). The partial pressure of carbon dioxide (pCO_2) is a function of respiration (Li et al. 2010) and ranges from 507 to 1843 μatm , which is one- to fivefold higher than the local atmospheric pCO_2 (averaging 410 μatm). The $\delta^{13}C_{DIC}$ values in the river were on average -8.7‰ and increased from -9.5‰ in the low-flow season to -7.5‰ in the high-flow season, thus showing distinct temporal variations.

Discussion

Controls on elemental content and discharge (C-Q) relationships

The C-Q relationship provides unique information on the interactions between dissolved solute contents and hydrological processes and can be modeled by a power law function (Diamond and Cohen 2018; Godsey et al. 2009; Koger et al. 2018; Musolff et al. 2015; Rose et al. 2018; Singley et al. 2017):

$$C = a \times Q^b \tag{1}$$

where the parameter *a* and slope *b* are constants, *b* represents the index of the deviation from chemostatic behaviors (Clow and Mast 2010). A value of *b* ≈ 0 indicates chemostatic behavior (Godsey et al. 2009), whereas if *b* ≈ -1, the solute content varies inversely with the discharge, and *C* is only controlled by *Q* (Godsey et al. 2009). Lastly, when *b* > 0, the solute contents increase with discharge (Musolff et al. 2015). C-Q relationships for the major ions (Ca²⁺, Mg²⁺, HCO₃⁻, and K⁺) exhibit significant chemostatic behaviors compared with Na⁺, Cl⁻, and SO₄²⁻, which are influenced by dilution effects

at various degrees, while the dissolved Si content yields a positive relationship with high discharge, which may indicate that multiple biogeochemical processes counteract the dilution effect by rainwater. The results for these various C-Q relationships are shown in Fig. 2.

The patterns exhibited by trace element contents in the case of discharge variabilities are different compared to those of the major ions (Baronas et al. 2017; Kirchner and Neal 2013). C-Q relationships for trace elements, like Sr, Al, Li, Zn, and Cu, present significant chemostatic behaviors responding to increasing discharge. Most elements (Ba, Sb, Mn, Mo, U, Pb, Co) display weakly negative correlations with increasing discharge (*R*² from 0.19 to 0.57), whereas Cr, Rb, Ni, and V show no distinct correlation with discharge change (Fig. 3).

The coefficient of variation of content and discharge (*CV_C*/*CV_Q*) provide a better understanding of the chemostatic/chemodynamic behavior of solute contents as a response to hydrological variabilities (Musolff et al. 2015; Thompson et al. 2011). This coefficient of variation reflects the sources and sinks of dissolved analytes and is defined by the following equation:

$$CV_C / CV_Q = (\mu_Q \sigma_C) / (\mu_C \sigma_Q) \tag{2}$$

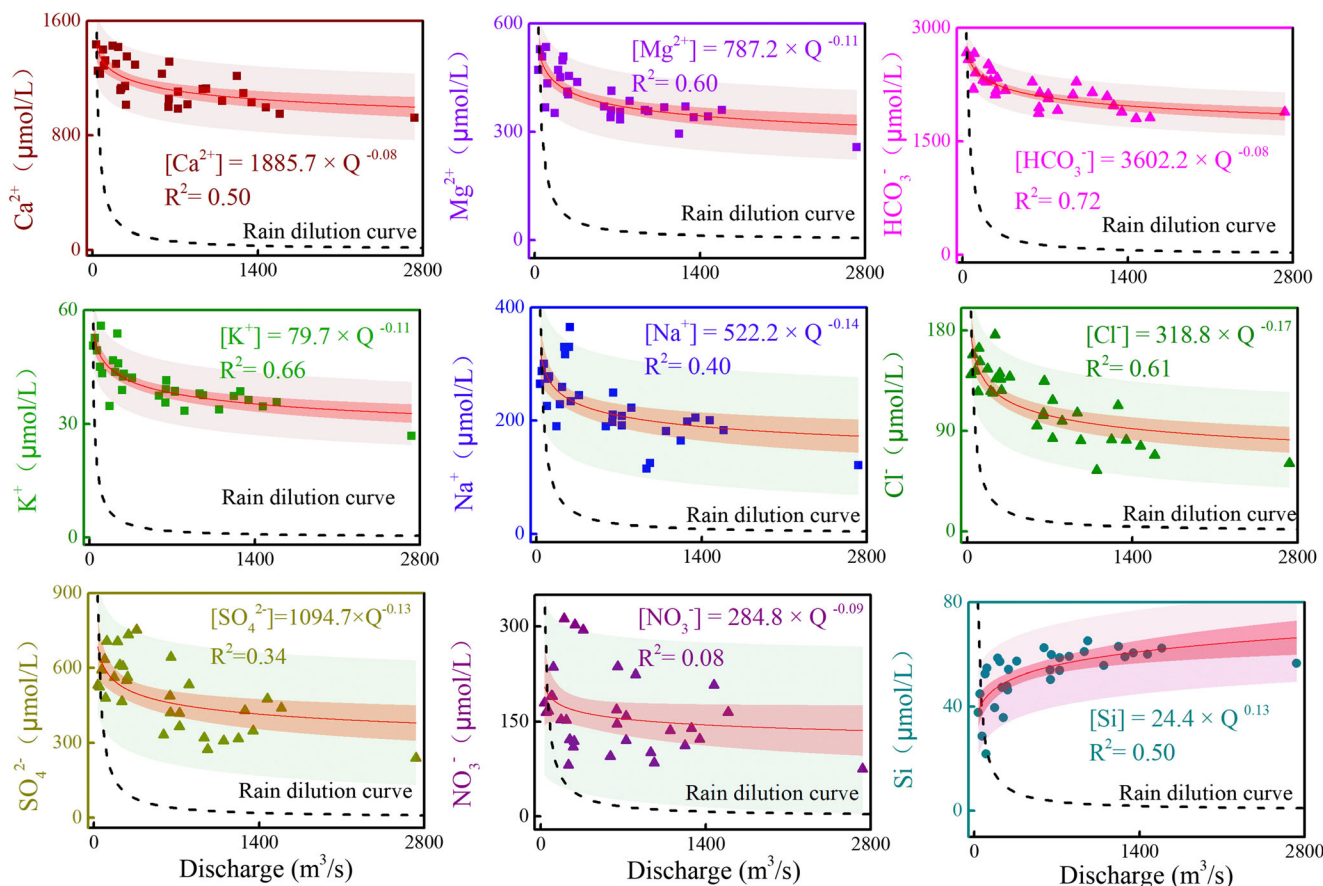


Fig. 2 Content–discharge relationship of solutes (K⁺, Na⁺, Ca²⁺, Mg²⁺, HCO₃⁻, Cl⁻, NO₃⁻, SO₄²⁻, and Si) in the Beipan River

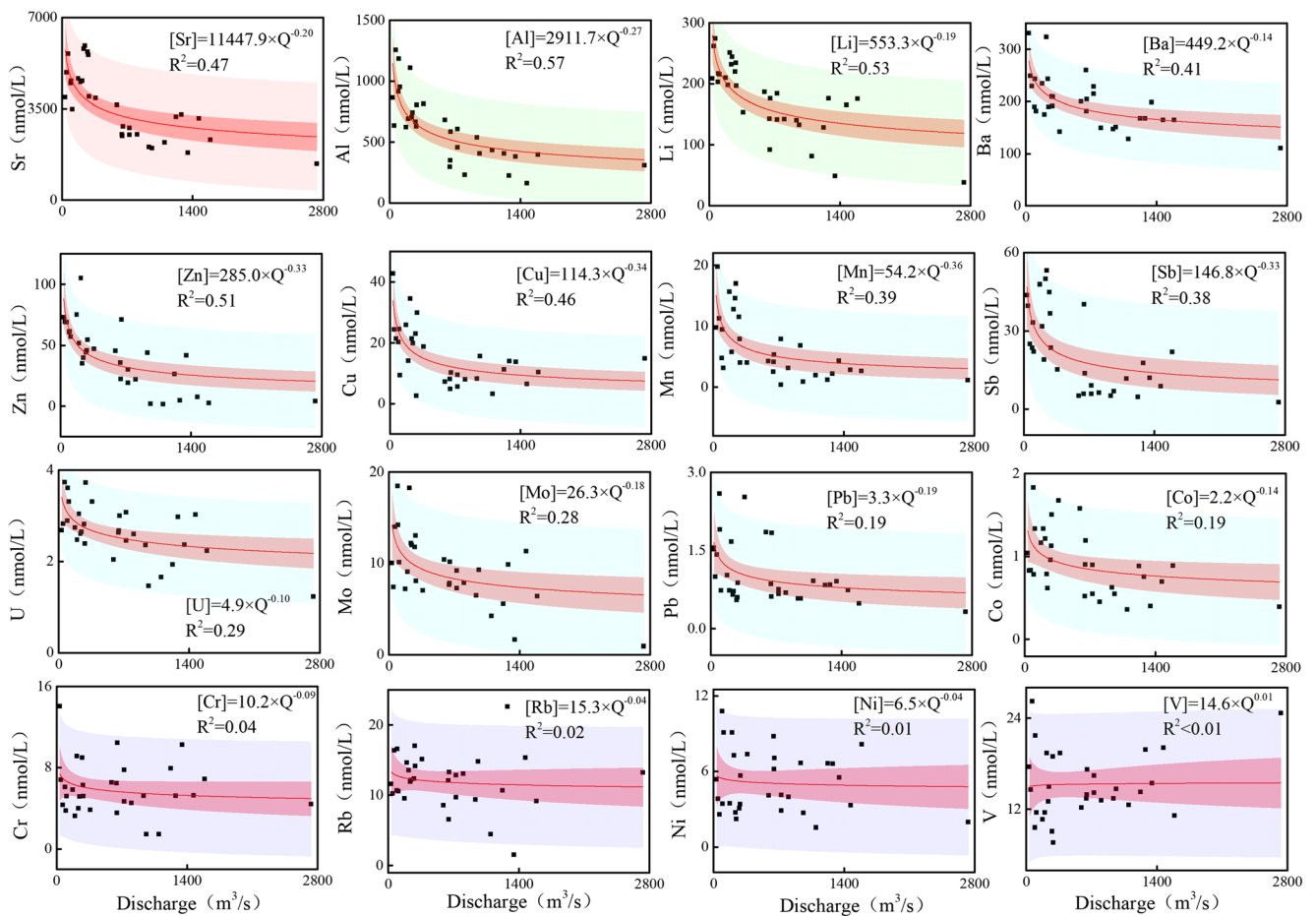


Fig. 3 Content–discharge relationship of the dissolved trace elements (Sr, Al, Li, Zn, Cu, Ba, Sb, Mn, Mo, U, Pb, Co, Cr, Rb, Ni, and V)

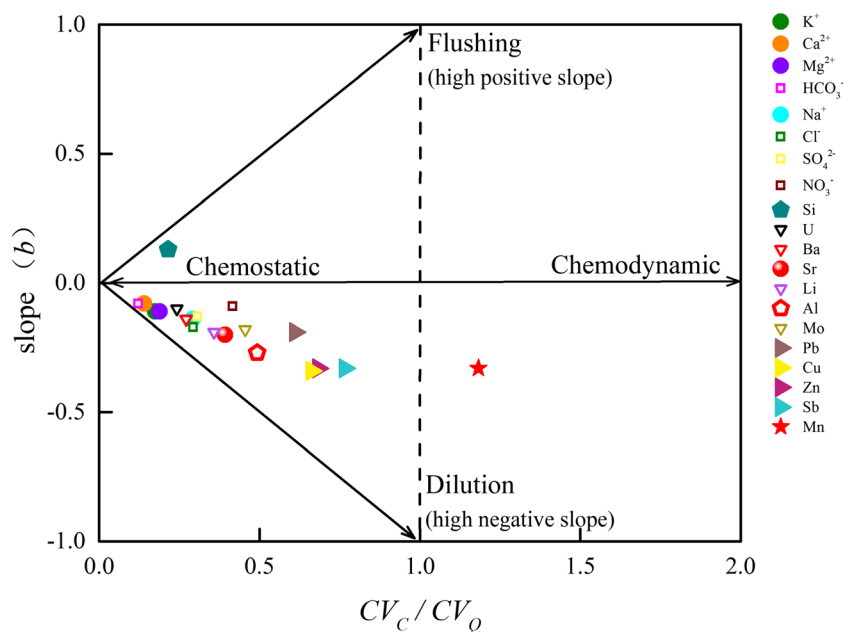
where CV is the coefficient of variation for dissolved solutes, expressed as the standard deviation σ divided by its average value μ (Zhong et al. 2018). According to Musolff et al. (2015), chemostatic behavior ($-0.2 < b < 0.2$ and $CV_D/CV_Q < 0.5$) is characterized by little solute content variations relative to discharge changes, while flushing behaviors are characterized by positive b values, and dilution behaviors are characterized by negative b values. Chemodynamic behavior ($b \approx 0$, $CV_D/CV_Q > 1$) is a discharge-independent state indicating that high content of dissolved solutes are not controlled by Q (Musolff et al. 2015; Zhong et al. 2018). As Ca^{2+} , Mg^{2+} , and Sr are mainly derived from carbonate weathering (Gaillardet et al. 1999), these elements show chemostatic behavior. U content in the study river is mainly sourced from carbonate weathering (Palmer and Edmond 1993; Wei et al. 2013) and shows a behavior similar to carbonate-sourced ions Ca^{2+} , Mg^{2+} , and HCO_3^- , all of which are highly influenced by the equilibrium of carbonate dissolution/precipitation processes (Tipper et al. 2006; Zhong et al. 2018; Zhong et al. 2017a; Zhong et al. 2017b). Silicate weathering is the primary source of Al and Li (Chen et al. 2014; Torres et al. 2015), both of which show significant effects from dilution akin to those of Na^+ . This indicates that silicate-sourced ions have relatively

higher sensitivity in response to hydrological variability compared to carbonate-sourced ions. Zn, Cu, Ba, Sb, Mn, Mo, and Pb are closely associated with human activities and therefore have inherited “anthropogenic overprints” (Chen et al. 2014). For example, Mn content exhibits a significant chemodynamic behavior (Fig. 4), which may be attributed to a potential mining source in the investigated catchment (Liu et al. 2017a; Qi and Yang 2011; Qing et al. 2008).

Sources for major and trace elements

Carbonates are distinguished by higher ratios of Ca/Na and Sr/Na compared to silicates (Gaillardet et al. 1999). A significantly positive relationship between Ca/Na ratios and discharge (Fig. 5a) exists, which indicates that carbonate weathering is a dominant contribution to dissolved loads in the investigated river, similar to previous findings (Qin et al. 2006; Tipper et al. 2006; Torres et al. 2015; Wei et al. 2013; Xu and Liu 2007). Meanwhile, in the high-flow season, river waters with higher Ca/Na ratios are generally yielded lower Sr/Na ratios, which suggests that the contribution to river chemistry from silicate weathering is greater in the high-flow season compared to those in the low-flow season (Wei

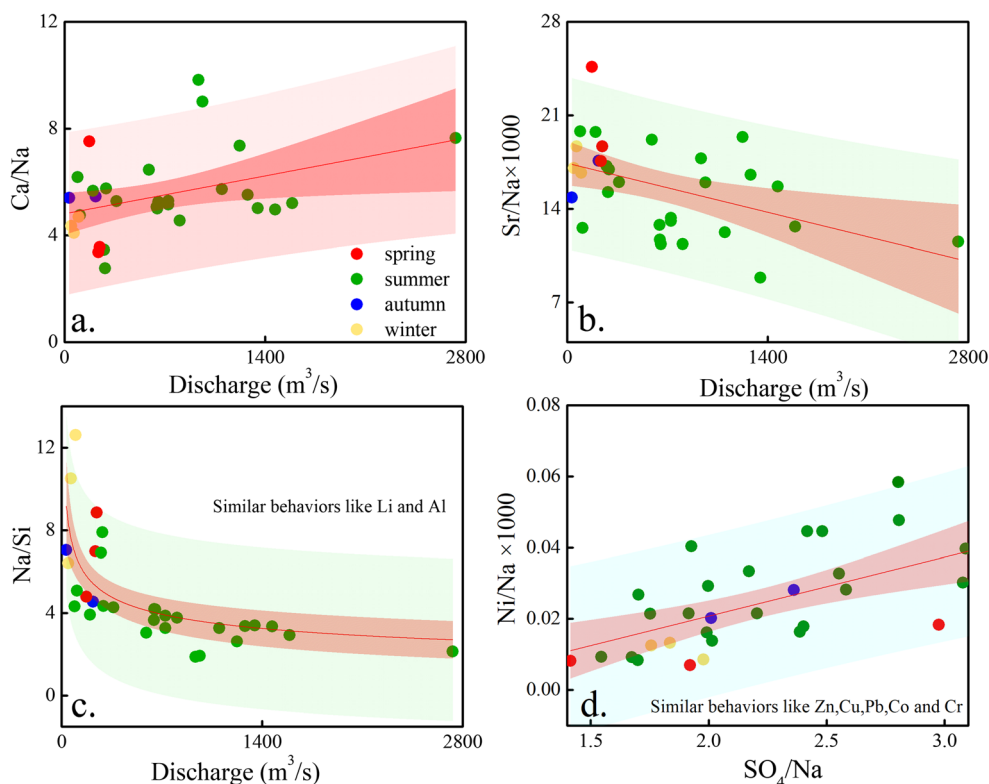
Fig. 4 Slope (b) vs. CV_c/CV_Q for dissolved solutes of the Beipan River



et al. 2013) (Fig. 5b). Na and Si are sourced from silicate weathering, and the variation in the Na/Si ratio with changes in discharge indicates that the Si content is maintained by balance between the precipitation of secondary silicates and weather of primary silicates (Fig. 5c), which is consistent with previous studies (Clow and Mast 2010; Torres et al. 2015; Zhong et al. 2017a; Zhong et al. 2017b). During the dissolution of silicates, both Na and Si are released into dissolved

loads. As dissolution occurs, saturation with secondary silicates buffers the dissolved Si content, but as Na is not readily partitioned into secondary silicates, its content continues to increase (Georg et al. 2006; Torres et al. 2015). Li and Al are derived from the same lithological source and display similar behaviors with Na. On the other hand, the seasonal variability of the ratios of silicate derived elements versus Si is characterized by higher ratios in the low-flow season, which

Fig. 5 Relationships between discharge and Ca/Na ratios (a), Sr/Na ratios (b), and Na/Si ratios (c) in different seasons and the correlation ratios of SO_4/Ca and $Ni/Na \times 1000$ (d) in the Beipan River



decrease more as a response to discharge than the high-flow season ratios (Fig. 5c). This may be explained by the fact that the silicate weathering in the low-flow season is dominated by long water–rock interaction time (Tipper et al. 2006; Torres et al. 2015; Zhong et al. 2017b).

The riverine sulfate might be influenced by various sources (sulfide oxidation, gypsum dissolution, and anthropogenic activities). Following high temporal resolution water chemistry and isotopic measurements, sulfuric acid has been shown to play a significant role in chemical weathering in investigated catchments (Li et al. 2008; Liu et al. 2017b). Interestingly, there is a significant positive relationship between the ratios of Ni/Na and SO₄/Na during the sampling period (Fig. 5d), which may indicate that sulfide minerals provide a key contribution to the behavior of Ni. Meanwhile, Zn, Cu, Pb, Co, and Cr display similar behaviors, and as these ions are generally enriched in minerals (Garzanti et al. 2011; Yang et al. 2009). These results may be related to the mining activities in this study catchment.

Impacts of climatic variability on chemical weathering fluxes

The temporal hydrological variability in the Guizhou Province, lying in the center of the Southeast Asian Karst Region, is affected by the seasonal monsoonal climate. According to the above discussion (the “Sources for major and trace elements” section) on the variation of element dynamics as a function of discharge, a forward model is run to estimate the relative contribution of various sources in the investigated river (see Eqs. 7 and 8). The results exhibit a wide range of flux values, with carbonate weathering fluxes (F_{carb}) ranging from 4.0–207.8 kg/s and silicate weathering fluxes (F_{sil}) from 0.3–11.4 kg/s, both of which having a significant positive correlation with discharge variability (Fig. 6). These positive correlations suggest that the hydrological condition is a dominant factor controlling the chemical weathering fluxes. The observed contours of the power law exponents represent

chemostatic behaviors, ranging from -1 (dilution) to 0 (chemostasis). Both F_{sil} and F_{carb} show strong chemostatic behaviors, and similar findings have also been observed for global rivers impacted by climatic variability (Szramek et al. 2007; Tipper et al. 2006; Zhong et al. 2018; Zhong et al. 2017a, 2017b). The dissolution kinetic characters in rapidly eroding environments may explain the near chemostatic behavior of chemical weathering fluxes, varying with changing discharge, especially for carbonate weathering (Tipper et al. 2006; Zhong et al. 2017b, 2018). The increase in erosion intensity during high discharge favored by the monsoonal climate conditions enhances the hydrological flushing, which induces the reaction of the mineral surface area and accelerates the weathering of minerals, thus allowing the more easily weathered carbonates to be dissolved (Clow and Mast 2010; Ollivier et al. 2010). So, this indicates that, in the study river, the chemical weathering fluxes with high discharge may have higher contributions from carbonate weathering.

Carbon dynamics impacted by climatic variabilities

Riverine DIC may originate from different endmembers and be modified by processes occurring due to changes in the water pathways (Li et al. 2008). The fluxes of DIC (F_{DIC}) in the study river present a strong positive relationship with discharge (Fig. 7a), and the power law exponents of F_{DIC} is close to 0, which indicates that the DIC fluxes in the Beipan River are dominated by hydrological conditions. Besides, the weathering of carbonates and silicates is mostly involved with the dissolution of biogenic CO₂, thus contributing to the DIC pool (Li et al. 2008; McClanahan et al. 2016).

$\delta^{13}C_{DIC}$ is a useful tool to trace the fluvial carbon sources and the biogeochemical processes. Normalized discharge (NQ) and normalized temperature (NT) are used to quantify the relative temporal discharge/temperature dynamics:

$$NQ = (Q_i - Q_{min}) / (Q_{max} - Q_{min}) \tag{3}$$

$$NT = (T_i - T_{min}) / (T_{max} - T_{min}) \tag{4}$$

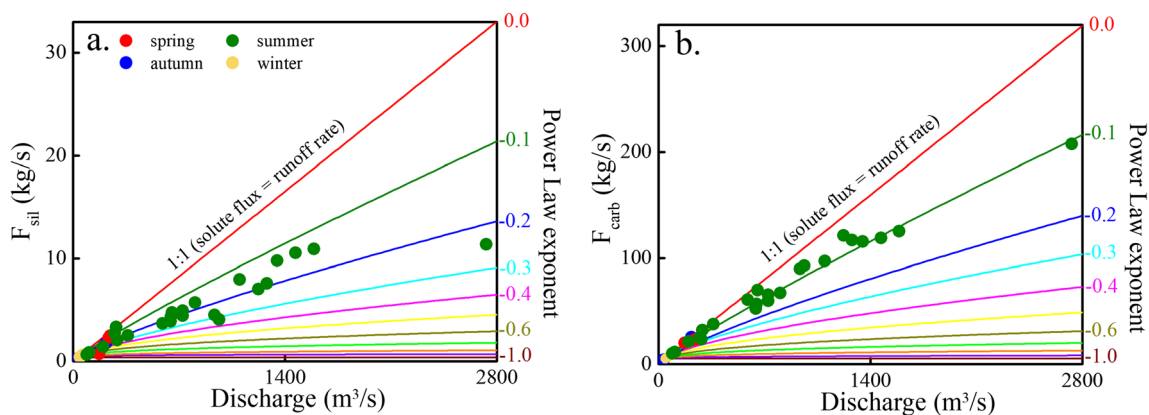


Fig. 6 Relationships between discharge and carbonate weathering fluxes (F_{carb}) (a), silicate weathering fluxes (F_{sil}) (b)

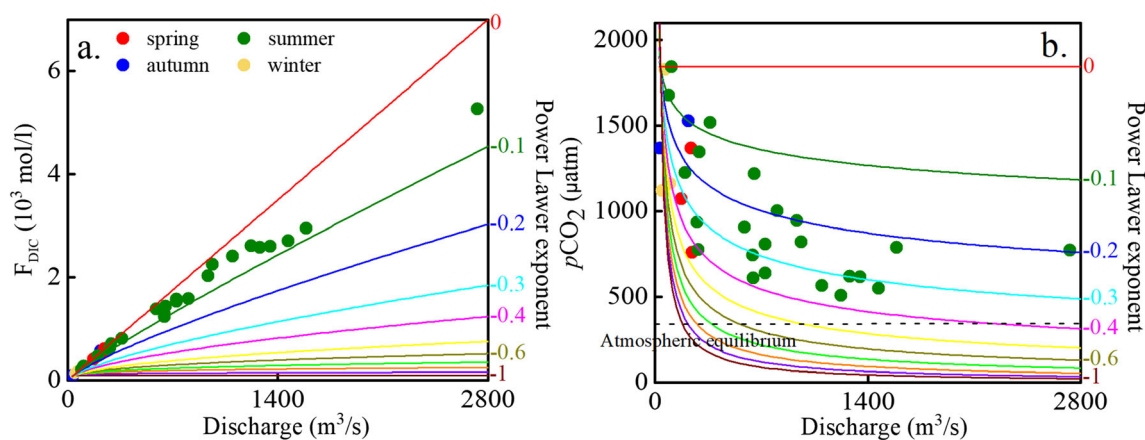


Fig. 7 Relationships between discharge and DIC weathering fluxes (F_{DIC}) (a) and $p\text{CO}_2$ (b) in the Beipan River

where Q_i and T_i represent, respectively, the instantaneous discharge rate and the water temperature rate at time i , and min and max represent the respective minimum and maximum value for discharge and temperature. The Beipan River presents positive relationships of $\delta^{13}\text{C}_{\text{DIC}}$ versus NQ and NT (Fig. 8a, b), which indicate that higher $\delta^{13}\text{C}_{\text{DIC}}$ are associated with higher discharge and temperature conditions, and $\delta^{13}\text{C}_{\text{DIC}}$ has higher sensitivity than riverine DIC with respect to increasing discharge (Waldron et al. 2007).

The difference between the measured and theoretical DIC values (from the theoretical dilution curve) is defined as ΔDIC (Zhong et al. 2018). Riverine DIC contents show chemostatic behavior with increasing discharge, indicating that large amounts of exogenous DIC are flushed into the river. The observed variations of $\delta^{13}\text{C}_{\text{DIC}}$ values are inversely related to seasonal changes in $p\text{CO}_2$ and ΔDIC content (Fig. 9a, b), which suggests that photosynthesis is the dominant control for the riverine DIC content in the high-flow season rather than during the low-flow season. During the high-flow season, high discharge changes the groundwater flow paths to shallow subsurface flow paths (Tipper et al. 2006), and high temperature could promote ecological processes, resulting in strong plants photosynthesis leading to the faster uptake of light carbon ^{12}C (Chen et al. 2017; Gammons et al. 2010; Liu et al. 2008). In addition, the $p\text{CO}_2$

values show significant chemostatic behavior in response to increasing discharge, especially during periods of the wet season when the discharge is greater than $700\text{ m}^3/\text{s}$ (Fig. 7b). This demonstrates that the biological CO_2 produced by microbiological activities and biological effects would be enhanced during the rainy season in southwestern China (McClanahan et al. 2016; Zhong et al. 2017b). Relative to the high-flow season, the decrease in $\delta^{13}\text{C}_{\text{DIC}}$ values during the low-flow season suggests that the dominant source of DIC added to the river water in this season is CO_2 from groundwater contribution, which has lower $\delta^{13}\text{C}_{\text{DIC}}$ values (Li et al. 2005, 2008).

The mixing model, IsoSource, is employed to calculate carbon sources based on $\delta^{13}\text{C}$ values of distinct DIC endmembers. According to previous studies in the research area (Li et al. 2008), the carbonate carbon ($\delta^{13}\text{C} = 0\text{‰}$) is entered into the model as a constant. The biological carbon is expected to be similar to that of dominant C_3 plants, considering a small diffusion fraction of soil CO_2 ($\sim 4\text{‰}$) to the atmosphere (Aucour et al. 1999; Cerling et al. 1991; Li et al. 2008), hence -22.6‰ for biological carbon. The source contributions to riverine DIC can be calculated as following:

$$\delta^{13}\text{C}_{\text{DIC}} = \delta^{13}\text{C}_{\text{carb}} \times a + \delta^{13}\text{C}_{\text{bio}} \times b \quad (5)$$

$$a + b = 1 \quad (6)$$

Fig. 8 Correlations between $\delta^{13}\text{C}$ values and NT (a) and NQ (b) in the Beipan River

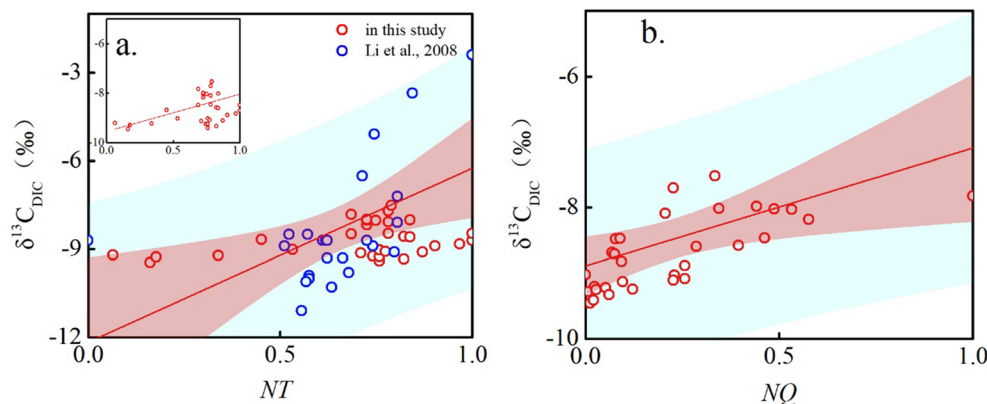
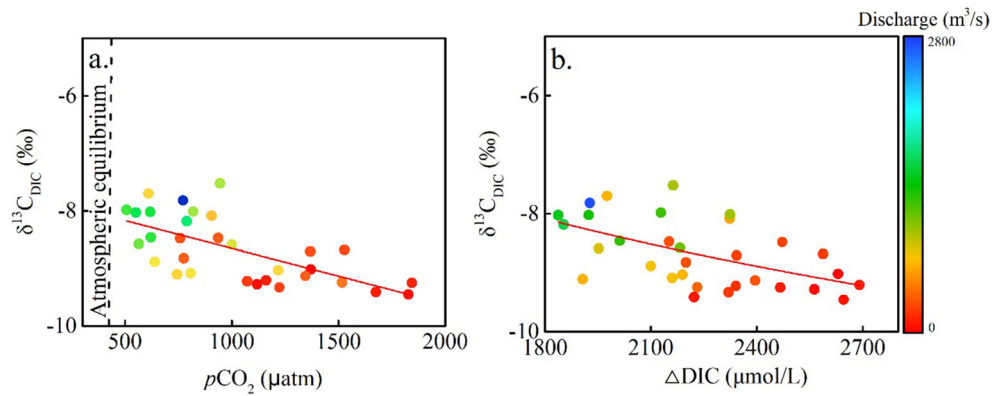


Fig. 9 Correlations between $\delta^{13}\text{C}$ values with $p\text{CO}_2$ (a) and ΔDIC (b) in the Beipan River



where $\delta^{13}\text{C}_{\text{carb}}$ and $\delta^{13}\text{C}_{\text{bio}}$ are the carbon isotopic values of carbonate (DIC_{carb}) and biological carbon (DIC_{bio}), respectively. And a and b are the proportions of carbon from carbonate and biological carbon sources, respectively. Based on the calculation, the contribution of DIC_{carb} ranges from 58% in the low-flow conditions to 67% in the high-flow conditions, with a mean value of 62%, and implies that carbonate weathering is the dominant controller on the chemostatic behavior of total riverine DIC with increasing discharge in the hydrological year; meanwhile, the contribution of DIC_{bio} increases from 33% in the low-flow conditions to 42% in the high-flow conditions, with a mean value of 28%, which also presents a strong chemostatic behavior with increasing discharge change, indicating that DIC_{bio} produced by microbiological activities and plant biological effects would be enhanced during the high-flow conditions in southwestern China, agree with previous studies (Li et al. 2010; Zhong et al. 2017b).

These results confirm that carbonate dissolution and involved ecosystem photosynthesis are the dominant processes controlling the riverine DIC in the study river. The CO_2 depletion owing to plant photosynthesis resulted in decrease of $p\text{CO}_2$ values and ΔDIC contents in the high-flow conditions in this study river.

Conclusions

The metabolism of multi-biogeochemical processes are mainly impacted by the observed temporal hydrological variations in the study river water, based on high-frequency variations in riverine major, trace elements, and $\delta^{13}\text{C}_{\text{DIC}}$ values in a hydrological year. Most elements contents show dilution effects responding to increasing discharge. However, due to the fast kinetic carbonate dissolution and biological processes, etc., they show significant chemostatic behavior responding to high discharge. The CO_2 depletion owing to plant photosynthesis resulted in a decrease in $p\text{CO}_2$ values and ΔDIC content. The increase in $\delta^{13}\text{C}_{\text{DIC}}$ confirms that plant photosynthesis is

the dominant process controlling DIC in the high-flow season. These results confirm that carbonate dissolution and the associated ecosystem photosynthesis/respiration are the dominant processes controlling the riverine DIC in the Beipan River. In addition, based on the mixing model IsoSource, it is shown that the contribution of carbonate weathering and biological carbon are the main sources to the total DIC in this study river. Thus, this work demonstrates that the well-established link between plant ecological processes and carbon dynamics in a typical karst river is impacted by monsoonal climate conditions.

Acknowledgements We deeply thank Dr. Si-Liang Li and Dr. Jun Zhong for their valuable comments that have largely improved the scientific writing of this paper, Dr. Fu-Jun Yue and Dr. Zhong-Jun Wang for their help in the field sampling, and the International Science Editing (<http://www.internationalscienceediting.com>) for editing this manuscript.

Funding information This work was supported financially by the National Natural Science Foundation of China (Grant No. 41807366), Guizhou Science and Technology Department Fund (Grant No. [2019]1043), Guizhou Education Department Fund (Grant No. [2018]161), and scientific platform talent project of Guizhou University of Finance and Economics (Grant No. [2018]5774-029).

Appendix

Calculation of silicate and carbonate weathering fluxes:

The fluxes of silicate weathering (F_{sil}) and carbonate weathering (F_{carb}) were calculated as follows:

$$F_{\text{sil}} = ([\text{K}]_{\text{sil}} \times M_{\text{k}} + [\text{Na}]_{\text{sil}} \times M_{\text{Na}} + [\text{Ca}]_{\text{sil}} \times M_{\text{Ca}} + [\text{Mg}]_{\text{sil}} \times M_{\text{Mg}} + [\text{Si}]_{\text{sil}} \times M_{\text{SiO}_2}) \times \text{Discharge} \quad (7)$$

$$F_{\text{carb}} = ([\text{Ca}]_{\text{carb}} \times M_{\text{Ca}} + [\text{Mg}]_{\text{carb}} \times M_{\text{Mg}}) \times \text{Discharge} \quad (8)$$

where M is the molar mass of the element.

References

- Amaral JHF, Borges AV, Melack JM, Sarmiento H, Barbosa PM, Kasper D, de Melo ML, De Fex-Wolf D, da Silva JS, Forsberg BR (2018) Influence of plankton metabolism and mixing depth on CO₂ dynamics in an Amazon floodplain lake. *Sci Total Environ* 630:1381–1393. <https://doi.org/10.1016/j.scitotenv.2018.02.331>
- Aucour A-M, Sheppard SMF, Guyomar O, Wattelet J (1999) Use of ¹³C to trace origin and cycling of inorganic carbon in the Rhône river system. *Chem Geol* 159(1–4):87–105. [https://doi.org/10.1016/S0009-2541\(99\)00035-2](https://doi.org/10.1016/S0009-2541(99)00035-2)
- Baronas JJ, Torres MA, Clark KE, West AJ (2017) Mixing as a driver of temporal variations in river hydrochemistry: 2. Major and trace element concentration dynamics in the Andes–Amazon transition. *Water Resour Res* 53(4):3120–3145. <https://doi.org/10.1002/2016WR019729>
- Brunet F, Dubois K, Veizer J, Nkoue Ndong GR, Ndam Ngoupayou JR, Boeglin JL, Probst JL (2009) Terrestrial and fluvial carbon fluxes in a tropical watershed: Nyong basin, Cameroon. *Chem Geol* 265(3–4):563–572. <https://doi.org/10.1016/j.chemgeo.2009.05.020>
- Cerling TE, Solomon DK, Quade J, Bowman JR (1991) On the isotopic composition of carbon in soil carbon dioxide. *Geochim Cosmochim Acta* 55(11):3403–3405. [https://doi.org/10.1016/0016-7037\(91\)90498-t](https://doi.org/10.1016/0016-7037(91)90498-t)
- Chen J-B, Gaillardet J, Bouchez J, Louvat P, Wang YN (2014) Anthropophile elements in river sediments: overview from the Seine River, France. *Geochem Geophys Geosyst* 15:4526–4546. <https://doi.org/10.1002/2014GC005516>
- Chen B, Yang R, Liu Z, Sun H, Yan H, Zeng Q, Zeng S, Zeng C, Zhao M (2017) Coupled control of land uses and aquatic biological processes on the diurnal hydrochemical variations in the five ponds at the Shewan Karst Test Site, China: implications for the carbonate weathering-related carbon sink. *Chem Geol* 456:58–71. <https://doi.org/10.1016/j.chemgeo.2017.03.006>
- Clow DW, Mast MA (2010) Mechanisms for chemostatic behavior in catchments: implications for CO₂ consumption by mineral weathering. *Chem Geol* 269(1–2):40–51. <https://doi.org/10.1016/j.chemgeo.2009.09.014>
- Colombo N, Gruber S, Martin M, Malandrino M, Magnani A, Godone D, Freppaz M, Fratianni S, Salerno F (2018) Rainfall as primary driver of discharge and solute export from rock glaciers: the Col d'Olen Rock Glacier in the NW Italian Alps. *Sci Total Environ* 639:316–330. <https://doi.org/10.1016/j.scitotenv.2018.05.098>
- Correa A, Breuer L, Crespo P, Céleri R, Feyen J, Birkel C, Silva C, Windhorst D (2019) Spatially distributed hydro-chemical data with temporally high-resolution is needed to adequately assess the hydrological functioning of headwater catchments. *Sci Total Environ* 651:1613–1626. <https://doi.org/10.1016/j.scitotenv.2018.09.189>
- Cox PM, Betts RA, Jones CD, Spall SA, Totterdell IJ (2000) Acceleration of global warming due to carbon-cycle feedbacks in a coupled climate model. *Nature* 408:184–187. <https://doi.org/10.1038/35047138>
- Dessert C, Dupré B, Gaillardet J, François LM, Allègre CJ (2003) Basalt weathering laws and the impact of basalt weathering on the global carbon cycle. *Chem Geol* 202(3–4):257–273. <https://doi.org/10.1016/j.chemgeo.2002.10.001>
- Diamond JS, Cohen MJ (2018) Complex patterns of catchment solute-discharge relationships for coastal plain rivers. *Hydrol Process* 32(3):388–401. <https://doi.org/10.1002/hyp.11424>
- Doctor DH, Kendall C, Sebestyen SD, Shanley JB, Ohte N, Boyer EW (2008) Carbon isotope fractionation of dissolved inorganic carbon (DIC) due to outgassing of carbon dioxide from a headwater stream. *Hydrol Process* 22(14):2410–2423. <https://doi.org/10.1002/hyp.6833>
- Duvert C, Butman DE, Marx A, Ribolzi O, Hutley LB (2018) CO₂ evasion along streams driven by groundwater inputs and geomorphic controls. *Nat Geosci* 11(11):813–818. <https://doi.org/10.1038/s41561-018-0245-y>
- Gaillardet J, Dupré B (2005) Trace element in river water: treatise on geochemistry. In: Drever JJ, Holland HD (eds) *Surface and ground water weathering and soils*. Elsevier, Turekian, pp 25–272
- Gaillardet J, Dupré B, Allegre CJ, Negrel P (1997) Chemical and physical denudation in the Amazon River basin. *Chem Geol* 142:141–173. [https://doi.org/10.1016/S0009-2541\(97\)00074-0](https://doi.org/10.1016/S0009-2541(97)00074-0)
- Gaillardet J, Dupré B, Louvat P, Allègre CJ (1999) Global silicate weathering and CO₂ consumption rates deduced from the chemistry of rivers. *Chem Geol* 159:3–30. [https://doi.org/10.1016/S0009-2541\(99\)00031-5](https://doi.org/10.1016/S0009-2541(99)00031-5)
- Gammons CH, Babcock JN, Parker SR, Poulson SR (2010) Diel cycling and stable isotopes of dissolved oxygen, dissolved inorganic carbon, and nitrogenous species in a stream receiving treated municipal sewage. *Chem Geol* 283:44–55. <https://doi.org/10.1016/j.chemgeo.2010.07.006>
- Garzanti E, Andò S, France-Lanord C, Censi P, Vignola P, Galy V, Lupker M (2011) Mineralogical and chemical variability of fluvial sediments 2. Suspended-load silt (Ganga–Brahmaputra, Bangladesh). *Earth Planet Sci Lett* 302(1–2):107–120. <https://doi.org/10.1016/j.epsl.2010.11.043>
- Georg RB, Reynolds BC, Frank M, Halliday AN (2006) Mechanisms controlling the silicon isotopic compositions of river waters. *Earth Planet Sci Lett* 249(3–4):290–306. <https://doi.org/10.1016/j.epsl.2006.07.006>
- Godsey SE, Kirchner JW, Clow DW (2009) Concentration-discharge relationships reflect chemostatic characteristics of US catchments. *Hydrol Process* 23(13):1844–1864. <https://doi.org/10.1002/hyp.7315>
- Han ZJ, Jin ZS (1996) *Hydrology of Guizhou Province*. Seismology Press, China
- Jiang H, Liu W, Zhao T, Sun H, Xu Z (2018) Water geochemistry of rivers draining karst-dominated regions, Guangxi province, South China: implications for chemical weathering and role of sulfuric acid. *J Asian Earth Sci* 163:152–162. <https://doi.org/10.1016/j.jseaes.2018.05.017>
- Juhlke TR, Van Geldern R, Huneau F, Garel E, Santoni S, Hemmerle H, Barth JAC (2019) Riverine carbon dioxide evasion along a high-relief watercourse derived from seasonal dynamics of the water-atmosphere gas exchange. *Sci Total Environ* 657:1311–1322. <https://doi.org/10.1016/j.scitotenv.2018.12.158>
- Kirchner JW, Neal C (2013) Universal fractal scaling in stream chemistry and its implications for solute transport and water quality trend detection. *Proc Natl Acad Sci USA* 110(30):12213–12218. <https://doi.org/10.1073/pnas.1304328110>
- Koger JM, Newman BD, Goering TJ (2018) Chemostatic behaviour of major ions and contaminants in a semiarid spring and stream system near Los Alamos, NM, USA. *Hydrol Process* 32(11):1709–1716. <https://doi.org/10.1002/hyp.11624>
- Krishna MS, Viswanadham R, Prasad MHK, Kumari VR, Sarma VVSS (2018) Export fluxes of dissolved inorganic carbon to the Northern Indian Ocean from the Indian monsoonal rivers. *Biogeosci Discuss* 16(2):505–519. <https://doi.org/10.5194/bg-2018-4>
- Li SY (2018) CO₂ oversaturation and degassing using chambers and a new gas transfer velocity model from the Three Gorges Reservoir surface. *Sci Total Environ* 640–641:908–920. <https://doi.org/10.1016/j.scitotenv.2018.05.345>
- Li SY, Bush RT (2015) Changing fluxes of carbon and other solutes from the Mekong River. *Sci Rep* 5:16005. <https://doi.org/10.1038/srep16005>
- Li Yung Lung JYS, Tank SE, Spence C, Yang D, Bonsal B, McClelland JW, Holmes RM (2018) Seasonal and geographic variation in dissolved carbon biogeochemistry of rivers draining to the Canadian

- Arctic Ocean and Hudson Bay. *J Geophys Res Biogeosci* 123(10): 3371–3386. <https://doi.org/10.1029/2018jg004659>
- Li S-L, Liu C-Q, Tao F-X, Lang Y-C, Han G-L (2005) Carbon biogeochemistry of ground water, Guiyang, Southwest China. *Groundwater* 43(4):494–499. <https://doi.org/10.1111/j.1745-6584.2005.0036.x>
- Li S-L, Calmels D, Han G, Gaillardet J, Liu C-Q (2008) Sulfuric acid as an agent of carbonate weathering constrained by $\delta^{13}\text{C}_{\text{DIC}}$: examples from Southwest China. *Earth Planet Sci Lett* 270(3–4):189–199. <https://doi.org/10.1016/j.epsl.2008.02.039>
- Li S-L, Liu C-Q, Li J, Lang Y-C, Ding H, Li L (2010) Geochemistry of dissolved inorganic carbon and carbonate weathering in a small typical karstic catchment of Southwest China: isotopic and chemical constraints. *Chem Geol* 277(3–4):301–309. <https://doi.org/10.1016/j.chemgeo.2010.08.013>
- Liu Z, Liu X, Liao C (2008) Daytime deposition and nighttime dissolution of calcium carbonate controlled by submerged plants in a karst spring-fed pool: insights from high time-resolution monitoring of physico-chemistry of water. *Environ Geol* 55(6):1159–1168. <https://doi.org/10.1007/s00254-007-1062-6>
- Liu J, Li S-L, Chen J-B, Zhong J, Yue F-J, Lang Y, Ding H (2017a) Temporal transport of major and trace elements in the upper reaches of the Xijiang River, SW China. *Environ Earth Sci* 76(7):299–217. <https://doi.org/10.1007/s12665-017-6625-6>
- Liu J, Li S-L, Zhong J, Zhu XT, Guo QJ, Lang YC, Han XK (2017b) Sulfate sources constrained by sulfur and oxygen isotopic compositions in the upper reaches of the Xijiang River, China. *Acta Geochimica* 36(4):611–618. <https://doi.org/10.1007/s11631-017-0175-1>
- Maher K, Chamberlain CP (2014) Hydrologic regulation of chemical weathering and the geologic carbon cycle. *Science* 343(6178): 1502–1504. <https://doi.org/10.1126/science.1250770>
- McClanahan K, Polk J, Groves C, Osterhoudt L, Grubbs S (2016) Dissolved inorganic carbon sourcing using $\delta^{13}\text{C}_{\text{DIC}}$ from a karst influenced river system. *Earth Surf Process Landf* 41(3):392–405. <https://doi.org/10.1002/esp.3856>
- Musolff A, Schmidt C, Selle B, Fleckenstein JH (2015) Catchment controls on solute export. *Adv Water Resour* 86:133–146. <https://doi.org/10.1016/j.advwatres.2015.09.026>
- Ollivier P, Hamelin B, Radakovitch O (2010) Seasonal variations of physical and chemical erosion: a three-year survey of the Rhone River (France). *Geochim Cosmochim Acta* 74(3):907–927. <https://doi.org/10.1016/j.gca.2009.10.037>
- Palmer MR, Edmond JM (1993) Uranium in river water. *Geochim Cosmochim Acta* 57:4947–4955. [https://doi.org/10.1016/00167037\(93\)90131-F](https://doi.org/10.1016/00167037(93)90131-F)
- Pant RR, Zhang F, Rehman FU, Wang G, Ye M, Zeng C, Tang H (2018) Spatiotemporal variations of hydrogeochemistry and its controlling factors in the Gandaki River Basin, Central Himalaya Nepal. *Sci Total Environ* 622–623:770–782. <https://doi.org/10.1016/j.scitotenv.2017.12.063>
- Poulson SR, Sullivan AB (2010) Assessment of diel chemical and isotopic techniques to investigate biogeochemical cycles in the upper Klamath River, Oregon, USA. *Chem Geol* 269:3–11. <https://doi.org/10.1016/j.chemgeo.2009.05.016>
- Qi C, Yang Y (2011) The geology and prospecting potentiality of Lida Sb deposit in Funing, Yunnan. *Yunnan Geol* 30(3):294–298 (in Chinese)
- Qin J, Huh Y, Edmond JM, Du G, Ran J (2006) Chemical and physical weathering in the Min Jiang, a headwater tributary of the Yangtze River. *Chem Geol* 227(1–2):53–69. <https://doi.org/10.1016/j.chemgeo.2005.09.011>
- Qing W-q, He M-f, Chen Y-p (2008) Improvement of flotation behavior of Mengzi lead-silver-zinc ore by pulp potential control flotation. *Trans Nonferrous Metals Soc China* 18(4):949–954. [https://doi.org/10.1016/s1003-6326\(08\)60164-8](https://doi.org/10.1016/s1003-6326(08)60164-8)
- Qu B, Zhang Y, Kang S, Sillanpää M (2019) Water quality in the Tibetan Plateau: major ions and trace elements in rivers of the “Water Tower of Asia”. *Sci Total Environ* 649:571–581. <https://doi.org/10.1016/j.scitotenv.2018.08.316>
- Rai SK, Singh SK, Krishnaswami S (2010) Chemical weathering in the plain and peninsular sub-basins of the Ganga: impact on major ion chemistry and elemental fluxes. *Geochim Cosmochim Acta* 74(8): 2340–2355. <https://doi.org/10.1016/j.gca.2010.01.008>
- Rose LA, Karwan DL, Godsey SE (2018) Concentration-discharge relationships describe solute and sediment mobilization, reaction, and transport at event and longer timescales. *Hydrol Process* 32(18): 2829–2844. <https://doi.org/10.1002/hyp.13235>
- Schulte P, van Geldern R, Freitag H, Karim A, Négrel P, Petelet-Giraud E, Probst A, Probst J-L, Telmer K, Veizer J, Barth JAC (2011) Applications of stable water and carbon isotopes in watershed research: weathering, carbon cycling, and water balances. *Earth Sci Rev* 109(1–2):20–31. <https://doi.org/10.1016/j.earscirev.2011.07.003>
- Shin WJ, Chung GS, Lee D, Lee KS (2011) Dissolved inorganic carbon export from carbonate and silicate catchments estimated from carbonate chemistry and $\delta^{13}\text{C}_{\text{DIC}}$. *Hydrol Earth Syst Sci* 15(8):2551–2560. <https://doi.org/10.5194/hess-15-2551-2011>
- Singley JG, Wlostowski AN, Bergstrom AJ, Sokol ER, Torrens CL, Jaros C, Wilson CE, Hendrickson PJ, Gooseff MN (2017) Characterizing hyporheic exchange processes using high-frequency electrical conductivity-discharge relationships on subhourly to interannual timescales. *Water Resour Res* 53(5):4124–4141. <https://doi.org/10.1002/2016wr019739>
- Szramek K, McIntosh JC, Williams EL, Kanduc T, Ogrinc N, Walter LM (2007) Relative weathering intensity of calcite versus dolomite in carbonate-bearing temperate zone watersheds: carbonate geochemistry and fluxes from catchments within the St. Lawrence and Danube river basins. *Geochim Geophys Geosyst* 8(4). doi: <https://doi.org/10.1029/2006gc001337>
- Tamooch F, Borges AV, Meysman FJR, Van Den Meersche K, Dehairs F, Merckx R, Bouillon S (2013) Dynamics of dissolved inorganic carbon and aquatic metabolism in the Tana River Basin, Kenya. *Biogeochemistry* 10:6911–6928. <https://doi.org/10.5194/bg-10-6911-2013>
- Thompson SE, Basu NB, Lascurain J, Aubeneau A, Rao PSC. (2011). Relative dominance of hydrologic versus biogeochemical factors on solute export across impact gradients. *Water Resour Res* 47(10). doi: <https://doi.org/10.1029/2010wr009605>
- Tipper ET, Bickle MJ, Galy A, West AJ, Pomiès C, Chapman HJ (2006) The short term climatic sensitivity of carbonate and silicate weathering fluxes: insight from seasonal variations in river chemistry. *Geochim Cosmochim Acta* 70(11):2737–2754. <https://doi.org/10.1016/j.gca.2006.03.005>
- Torres MA, West AJ, Clark KE (2015) Geomorphic regime modulates hydrologic control of chemical weathering in the Andes–Amazon. *Geochim Cosmochim Acta* 166:105–128. <https://doi.org/10.1016/j.gca.2015.06.007>
- Viers J, Oliva P, Dandurand J-L, Dupré B, Gaillardet J (2014) Chemical weathering rates, CO_2 consumption, and control parameters deduced from the chemical composition of Rivers. *Treatise on Geochemistry* 175–194. <https://doi.org/10.1016/B978-0-08-095975-7.00506-4>
- Voss BM, Peucker-Ehrenbrink B, Eglinton TI, Fiske G, Wang ZA, Hoering KA, Montluçon DB, LeCroy C, Pal S, Marsh S, Gillies SL, Janmaat A, Bennett M, Downey B, Fanslau J, Fraser H, Macklam-Harron G, Martinec M, Wiebe B (2014) Tracing river chemistry in space and time: dissolved inorganic constituents of the Fraser River, Canada. *Geochim Cosmochim Acta* 124:283–308. <https://doi.org/10.1016/j.gca.2013.09.006>
- Waldron S, Scott EM, Soulsby C (2007) Stable isotope analysis reveals lower-order river dissolved inorganic carbon pools are highly

- dynamic. *Environ Sci Technol* 41:6156–6162. <https://doi.org/10.1021/es0706089>
- Wei G, Ma J, Liu Y, Xie L, Lu W, Deng W, Ren Z, Zeng T, Yang Y (2013) Seasonal changes in the radiogenic and stable strontium isotopic composition of Xijiang River water: implications for chemical weathering. *Chem Geol* 343:67–75. <https://doi.org/10.1016/j.chemgeo.2013.02.004>
- Xu ZF, Liu C-Q (2007) Chemical weathering in the upper reaches of Xijiang River draining the Yunnan–Guizhou Plateau, Southwest China. *Chem Geol* 239(1–2):83–95. <https://doi.org/10.1016/j.chemgeo.2006.12.008>
- Yang SY, Wang ZB, Guo Y, Li CX, Cai JG (2009) Heavy mineral compositions of the Changjiang (Yangtze River) sediments and their provenance-tracing implication. *J Asian Earth Sci* 35(1):56–65. <https://doi.org/10.1016/j.jseas.2008.12.002>
- Zakharova EA, Pokrovsky OS, Dupré B, Zaslavskaya MB (2005) Chemical weathering of silicate rocks in Aldan Shield and Baikal Uplift: insights from long-term seasonal measurements of solute fluxes in rivers. *Chem Geol* 214(3–4):223–248. <https://doi.org/10.1016/j.chemgeo.2004.10.003>
- Zhong J, Li S-L, Tao F, Ding H, Liu J (2017a) Impacts of hydrologic variations on chemical weathering and solute sources in the Min River basin, Himalayan-Tibetan region. *Environ Sci Pollut Res* 24(23):19126–19137. <https://doi.org/10.1007/s11356-017-9584-2>
- Zhong J, Li S-L, Tao F, Yue F, Liu CQ (2017b) Sensitivity of chemical weathering and dissolved carbon dynamics to hydrological conditions in a typical karst river. *Sci Rep* 7:42944–42949. <https://doi.org/10.1038/srep42944>
- Zhong J, Li S-L, Liu J, Ding H, Sun XL, Xu S, Wang TJ, Ellam RM, Liu C-Q (2018) Climate variability controls on CO₂ consumption fluxes and carbon dynamics for monsoonal rivers: evidence from Xijiang River, Southwest China. *J Geophys Res Biogeosci* 123(8):2553–2567. <https://doi.org/10.1029/2018jg004439>

Publisher's note Springer Nature remains neutral with regard to jurisdictional claims in published maps and institutional affiliations.